


Article

Solubility, Hansen Solubility Parameters and Thermodynamic Behavior of Emtricitabine in Various (Polyethylene Glycol-400 + Water) Mixtures: Computational Modeling and Thermodynamics

Faiyaz Shakeel, Nazrul Haq, Ibrahim A. Alsarra and Sultan Alshehri * 

Department of Pharmaceutics, College of Pharmacy, King Saud University, P.O. Box 2457, Riyadh 11451, Saudi Arabia; fsahmad@ksu.edu.sa (F.S.); nhaq@ksu.edu.sa (N.H.); ialsarra@ksu.edu.sa (I.A.A.)

* Correspondence: salshehri1@ksu.edu.sa

Received: 11 March 2020; Accepted: 28 March 2020; Published: 28 March 2020



Abstract: This study was aimed to find out the solubility, thermodynamic behavior, Hansen solubility parameters and molecular interactions of an antiviral drug emtricitabine (ECT) in various “[polyethylene glycol-400 (PEG-400) + water]” mixtures. The solubility of ECT in mole fraction was determined at “ $T = 298.2$ to 318.2 K” and “ $p = 0.1$ MPa” using an isothermal method. The experimental solubilities of ECT in mole fraction were validated and correlated using various computational models which includes “Van’t Hoff, Apelblat, Yalkowsky-Roseman, Jouyban-Acree and Jouyban-Acree-Van’t Hoff models”. All the models performed well in terms of model correlation. The solubility of ECT was increased with the raise in temperature in all “PEG-400 + water” mixtures studied. The highest and lowest solubility values of ECT were found in pure PEG-400 (1.45×10^{-1}) at “ $T = 318.2$ K” and pure water (7.95×10^{-3}) at “ $T = 298.2$ K”, respectively. The quantitative values of activity coefficients indicated higher interactions at molecular level in ECT and PEG-400 combination compared with ECT and water combination. “Apparent thermodynamic analysis” showed an “endothermic and entropy-driven dissolution” of ECT in all “PEG-400 + water” combinations studied. The solvation nature of ECT was found an “enthalpy-driven” in each “PEG-400 + water” mixture studied.

Keywords: computational modeling; cosolvent; emtricitabine; solubility; solubility parameter; thermodynamics

1. Introduction

Chemically, emtricitabine (ECT) is 5-fluoro-1-(2*R*,5*S*)-[2-(hydroxymethyl)-1,3-oxathiolan-5-yl]cytosine (Figure 1) [1]. Its molecular formula, molar mass and CAS registry number are $C_8H_{10}FN_3O_3S$, $247.24 \text{ g mol}^{-1}$ and 143491-54-7, respectively [1,2].

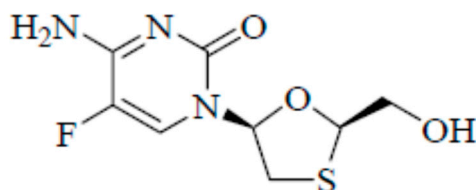


Figure 1. Chemical structure of emtricitabine (ECT).

It is a potential inhibitor of human immunodeficiency virus type I (HIV-I) reverse transcriptase and, hence, found to be effective against HIV-I infected patients [1,3]. ECT is prescribed to treat HIV-I

infected patients either alone or in combination with other antiviral agents [3–5]. ECT is marketed as Emtriva® in the treatment of HIV-I infected patients [1,5]. It has been found freely soluble in water at room temperature and, hence, its oral solution is available in the market [1]. It is extensively and rapidly absorbed by oral administration of capsules or oral solution due to its higher aqueous solubility [5]. The solubilities and other physicochemical parameters of ECT are poorly reported in literature. The solubility profiles and physicochemical properties of drugs and pharmaceuticals in cosolvent–water mixtures have greater impact for drug discovery process and formulation design [6–8]. Therefore, such physicochemical properties of ECT in cosolvent–water mixtures should be evaluated properly in order to obtain its complete physicochemical profile [6,7]. “Polyethylene glycol-400 (PEG-400)” has been reported as an efficient cosolvent in solubilization of drugs in aqueous media and it is miscible with water in all proportions [9–11]. The potential of PEG-400 has been studied extensively in solubility enhancement of various drugs [9–18]. Several formulation approaches including “3D printed controlled release tablets [4], film coated tablets [19], rapidly disintegrating vaginal tablets [20], immediate release tablets [21], vaginal gels [22], liposomal gels [23], microparticulate drug delivery system [24], nanosuspensions [25,26] and polymeric nanoparticles [5,27,28]” were reported to improve antiviral therapy and pharmacokinetic profile of ECT. The equilibrium solubility of ECT in water was found as 112 mg mL⁻¹ at “ $T = 298.2\text{ K}$ ” [1]. Nevertheless, the solubilities of ECT in different “PEG-400 + water” mixtures have not been reported in literature so far. Hence, this study was aimed to find out the solubility, Hansen solubility parameters, solution thermodynamics and solute–solvent molecular interactions of ECT in various “PEG-400 + water” mixtures, including mono solvents at “ $T = 298.2$ to 318.2 K ” and “ $p = 0.1\text{ MPa}$ ”. The effect of pressure on ECT solubility was not evaluated in the current work and; therefore, current work was performed at fixed air pressure (i.e., “ $p = 0.1\text{ MPa}$ ”). The investigated temperature ranges of “ $T = 298.15\text{ K}$ to 318.15 K ” were selected randomly with the interval of 5.0 K in such a manner that the highest studied temperature (i.e., “ $T = 318.2\text{ K}$ ”) should not exceed the fusion temperature of ECT and boiling points of the investigated solvents (i.e., water and PEG-400 in this case) [6,29]. The fusion temperature of ECT was obtained as 427.80 K by thermal analysis. The boiling temperatures of water and PEG-400 are 373.20 and 563.20 K, respectively. The highest studied temperature “ $T = 318.2\text{ K}$ ” was much lower than fusion temperature of ECT and boiling temperatures of water and PEG-400 and therefore the above temperature range was chosen in the current research. Experimental solubility values of ECT were correlated with five different computational models namely “Van’t Hoff, Apelblat, Yalkowsky-Roseman, Jouyban-Acree and Jouyban-Acree-Van’t Hoff models”. The solubility data and other physicochemical properties of ECT recorded in this study would be beneficial in “drug discovery process and dosage form design of ECT”.

2. Results and Discussion

2.1. Solid State Characterization of ECT

The solid state characterization of ECT in pure and equilibrated sample was conducted using X-ray diffraction (XRD) analysis. The XRD patterns of pure and equilibrated ECT are presented in Figure 2. The XRD patterns of pure ECT showed various characteristics peaks of ECT at $2\theta = 6.70^\circ$, 12.40° , 13.70° , 15.60° , 17.90° , 19.60° , 20.60° , 22.10° , 24.00° , 26.00° , 29.30° , 30.60° and 32.20° (Figure 2A). The characteristics peaks at various 2θ values suggested the crystallinity of the pure ECT. The XRD patterns of equilibrated ECT (recovered from pure water) also showed almost the same characteristic peaks at various 2θ values (Figure 2B). The results of XRD analysis also showed that ECT was not transformed into polymorphs/hydrates/solvates after saturation. Overall, the XRD spectra of pure and equilibrated ECT suggested that the physical form of the ECT remained unchanged after solubility experiments [29].

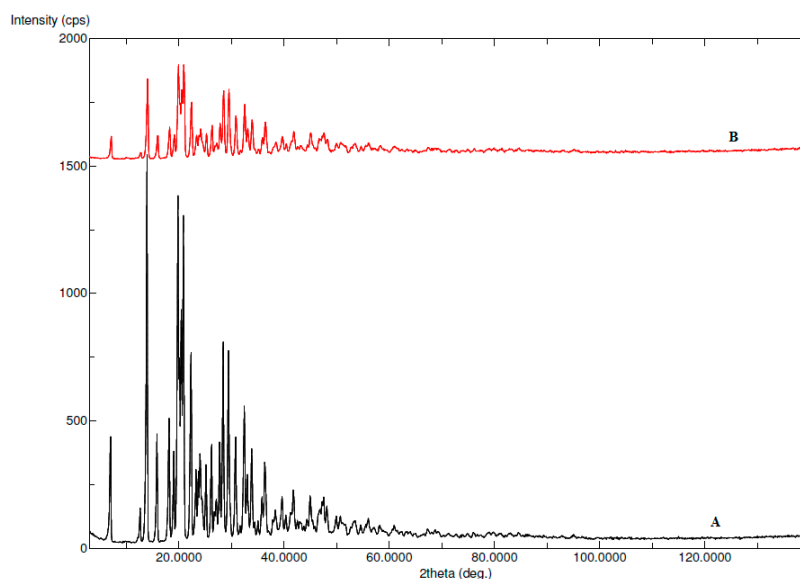


Figure 2. X-ray diffraction pattern (XRD) spectra of (A) pure ECT and (B) equilibrated ECT (recovered from pure water).

2.2. Solubility Data of ECT in Various “PEG-400 + Water” Mixtures

The experimental mole fraction solubilities of ECT (x_e) in different “PEG-400 + water” combinations and mono solvents at “ $T = 298.2$ to 318.2 K” and “ $p = 0.1$ MPa” were calculated using Equations (1) and (2) and results are summarized in Table 1.

Table 1. Experimental solubilities (x_e) of emtricitabine (ECT) in mole fraction in various “polyethylene glycol-400 (PEG-400) + water” mixtures (m) at “ $T = 298.2$ to 318.2 K” and “ $p = 0.1$ MPa”^a.

m	x_e				
	$T = 298.2$ K	$T = 303.2$ K	$T = 308.2$ K	$T = 313.2$ K	$T = 318.2$ K
0.0	7.95×10^{-3}	8.74×10^{-3}	9.53×10^{-3}	1.05×10^{-2}	1.15×10^{-2}
0.1	1.01×10^{-2}	1.11×10^{-2}	1.19×10^{-2}	1.30×10^{-2}	1.44×10^{-2}
0.2	1.31×10^{-2}	1.41×10^{-2}	1.54×10^{-2}	1.70×10^{-2}	1.84×10^{-2}
0.3	1.70×10^{-2}	1.88×10^{-2}	2.02×10^{-2}	2.22×10^{-2}	2.39×10^{-2}
0.4	2.27×10^{-2}	2.48×10^{-2}	2.68×10^{-2}	2.92×10^{-2}	3.20×10^{-2}
0.5	2.95×10^{-2}	3.21×10^{-2}	3.47×10^{-2}	3.78×10^{-2}	4.12×10^{-2}
0.6	3.81×10^{-2}	4.17×10^{-2}	4.50×10^{-2}	4.84×10^{-2}	5.30×10^{-2}
0.7	4.95×10^{-2}	5.41×10^{-2}	5.80×10^{-2}	6.26×10^{-2}	6.82×10^{-2}
0.8	6.33×10^{-2}	6.90×10^{-2}	7.43×10^{-2}	7.98×10^{-2}	8.68×10^{-2}
0.9	8.28×10^{-2}	9.01×10^{-2}	9.69×10^{-2}	1.03×10^{-1}	1.11×10^{-1}
1.0	1.06×10^{-1}	1.16×10^{-1}	1.25×10^{-1}	1.33×10^{-1}	1.45×10^{-1}
x_e^{idl}	3.74×10^{-2}	4.35×10^{-2}	5.05×10^{-2}	5.85×10^{-2}	6.76×10^{-2}

^a The standard uncertainties u are $u(T) = 0.13$ K, $u_r(m) = 0.10$ %, $u(p) = 0.003$ MPa and $u_r(x_e) = 1.10$ %.

The solubility of ECT in various “PEG-400 + water” combinations including mono solvents at different temperatures is not reported elsewhere. However, the equilibrium solubility of ECT in pure water at “ $T = 298.2$ K” has been reported as 112 mg mL^{-1} (converted to 8.09×10^{-3} in mole fraction) [1]. The mole fraction solubility of ECT in pure water at “ $T = 298.2$ K” was obtained as 7.95×10^{-3} in this study (Table 1). The recorded solubility of ECT in pure water “ $T = 298.2$ K” was very close to its literature value [1]. The reliability of the method was verified by determining the mole fraction solubility of isatin in pure water at $T = 298.2$ K and $T = 318.2$ K. The mole fraction solubility of isatin in pure water at $T = 298.2$ K and $T = 318.2$ K has been reported as 5.14×10^{-5} and 1.13×10^{-4} , respectively [11]. The mole fraction solubility of isatin in water at $T = 298.2$ K and $T = 318.2$ K was

found as 5.12×10^{-5} and 1.16×10^{-4} , respectively in this study. These results showed that the solubility of isatin in water recorded using the present method was much closed with its literature values [11]. Hence, the current method of solubility determination was accurate and reliable for the determination of ECT solubility. In general, the x_e values of ECT were found to enhance linearly with increase in temperature in all “PEG-400 + water” combinations and the x_e value of ECT was increased as the fraction of PEG-400 in “PEG-400 + water” mixtures increased ($p < 0.05$). Highest x_e of ECT was recorded in pure PEG-400 (1.45×10^{-1} at “ $T = 318.2$ K”), whereas, the lowest one was observed in pure water (7.95×10^{-3} at “ $T = 298.2$ K”). Highest x_e of ECT in pure PEG-400 could be possible due to lower polarity and lower Hansen solubility parameter (HSP) of PEG-400 in comparison with same physicochemical parameters of water [7,29]. The impact of mass fraction value of PEG-400 (m) on the solubility of ECT at “ $T = 298.2$ to 318.2 K” was also investigated and resulting data is summarized in Figure 3. The results indicated significant increase in the solubility of ECT with increase in m value of PEG-400 in “PEG-400 + water” mixtures at “ $T = 298.2$ to 318.2 K” ($p < 0.05$). In this study the influence of molar mass of PEGs on the solubility of ECT was not studied because only PEG-400 (average molar mass = 400 g mol^{-1}) was studied in this work. Nevertheless, it is well known that the solubility of solute in mole fraction is enhanced with increase in the molar mass of the solutes and the solvents. Hence, in this case, the solubility of ECT in mole fraction would be increased with increase in the molar mass of PEGs [30]. This observation is possible due to the fact that the solubility of ECT in mole fraction is inversely proportional to the mole fraction of the PEGs. It was also found that the solubility of ECT enhanced significantly from pure water to pure PEG-400 ($p < 0.05$). Therefore, PEG-400 can be applied as a physiologically compatible cosolvent in solubilization of ECT in water. Overall, the solubility of ECT in pure water, pure PEG-400 and various “PEG-400 + water” combinations was found good.

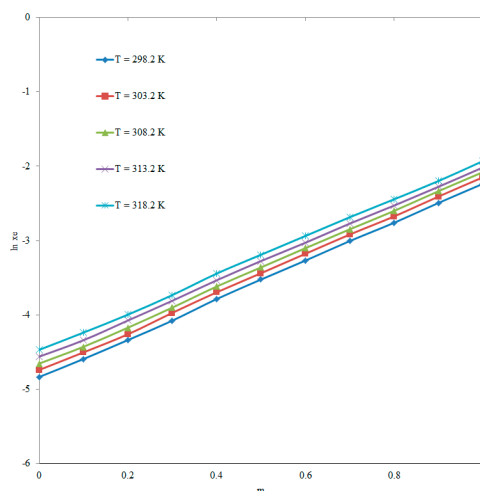


Figure 3. Effect of mass fraction (m) value of the PEG-400 on the solubility of ECT at “ $T = 298.2$ to 318.2 K”.

2.3. HSPs for ECT and Various “PEG-400 + Water” Mixtures

The HSPs for ECT, pure PEG-400 and pure water were calculated using “HSPiP software”. The HSPs of ECT, pure PEG-400 and pure water were calculated using Equation (3). However, the HSP of various “PEG-400 + water” mixtures free of ECT was calculated using Equation (4). The total HSP for ECT (δ) was calculated as $25.90 \text{ MPa}^{1/2}$. The value of total HSP for pure PEG-400 (δ_1) and pure water (δ_2) were calculated as 18.90 and $47.80 \text{ MPa}^{1/2}$, respectively. The value of HSP for various “PEG-400 + water” mixtures free of ECT (δ_{mix}) was estimated by applying Equation (4) and these values are presented in Table 2.

Table 2. Hansen solubility parameters ($\delta_{\text{mix}}/\text{MPa}^{1/2}$) for different “PEG-400 + water” combinations free of ECT at “ $T = 298.2 \text{ K}$ ”.

m	$\delta_{\text{mix}}/\text{MPa}^{1/2}$
0.1	44.91
0.2	42.02
0.3	39.13
0.4	36.24
0.5	33.35
0.6	30.46
0.7	27.57
0.8	24.68
0.9	21.79

The values of δ_{mix} for various “PEG-400 + water” combinations were found as 21.79 to 44.91 $\text{MPa}^{1/2}$. Overall, the HSP of pure PEG-400 ($\delta_1 = 18.90 \text{ MPa}^{1/2}$) and “PEG-400 + water” (at $m = 0.6$ to 0.9 ; $\delta_{\text{mix}} = 21.79$ to $30.46 \text{ MPa}^{1/2}$) were found to have close value with that of ECT ($\delta = 25.90 \text{ MPa}^{1/2}$). Overall, the results of HSPs were found in good agreement with experimental solubility values of ECT in various “PEG-400 + water” combinations.

2.4. Ideal Solubilities and Activity Coefficients

The ideal solubility (x^{idl}) of ECT at “ $T = 298.2$ to 318.2 K ” was obtained by applying Equation (5) and resulting values are summarized in Table 1. The x^{idl} values of ECT were observed as 3.74×10^{-2} to 6.76×10^{-2} at “ $T = 298.2$ to 318.2 K ”. The x^{idl} values of ECT were significantly higher than its x_e values in pure water ($p < 0.05$). However, the x^{idl} values of ECT were significantly lower than its x_e values in pure PEG-400 ($p < 0.05$) at each temperature evaluated. While, the x^{idl} values of ECT were more closed with its x_e values in various “PEG-400 + water” mixtures ($p > 0.05$). Due to maximum solubility of ECT in PEG-400, it could be applied as “an ideal cosolvent” for solubilization of ECT.

The “activity coefficient (γ_i)” for ECT in various “PEG-400 + water” mixtures at “ $T = 298.2$ to 318.2 K ” were estimated by applying Equation (6) and resulting data is summarized in Table 3. The γ_i values for ECT were observed highest in pure water compared with pure PEG-400 and various “PEG-400 + water” mixtures at every temperature evaluated. While, the γ_i values for ECT were found lowest in pure PEG-400 at every temperature evaluated. The γ_i values were found < 1.0 at $m = 0.6$ to 0.9 and pure PEG-400. The γ_i values for ECT were found to reduce rapidly from pure water to pure PEG-400 ($p < 0.05$). The highest γ_i of ECT in pure water could be possible due to the lowest solubility of ECT in water and higher dielectric constant/polarity of water compared with the highest solubility of ECT in PEG-400 and lower dielectric constant/polarity of neat PEG-400 [15,17]. The results of activity coefficients for ECT in various “PEG-400 + water” mixtures were found in accordance with their dielectric constants and mole fraction solubility [15]. Based on these results, the maximum solute–solvent interactions were found in ECT-PEG-400 compared with ECT-water.

Table 3. Activity coefficients (γ_i) of ECT in various “PEG-400 + water” mixtures (m) at “ $T = 298.2$ to 318.2 K”.

m	γ_i				
	$T = 298.2$ K	$T = 303.2$ K	$T = 308.2$ K	$T = 313.2$ K	$T = 318.2$ K
0.0	4.71	4.99	5.31	5.60	5.91
0.1	3.70	3.94	4.24	4.49	4.68
0.2	2.87	3.09	3.28	3.44	3.68
0.3	2.21	2.31	2.50	2.64	2.83
0.4	1.65	1.75	1.88	2.01	2.12
0.5	1.27	1.36	1.46	1.55	1.64
0.6	0.98	1.05	1.12	1.21	1.28
0.7	0.75	0.80	0.87	0.93	0.99
0.8	0.59	0.63	0.68	0.73	0.77
0.9	0.45	0.48	0.52	0.57	0.60
1.0	0.35	0.37	0.40	0.43	0.46

2.5. Thermodynamic Parameters of ECT

The values of various apparent thermodynamic parameters for dissolution behavior of ECT in different “PEG-400 + water” mixtures and pure solvents were obtained by applying van’t Hoff and Gibbs Equations (7–10) and results are summarized in Table 4. The values of apparent standard enthalpies ($\Delta_{\text{sol}}H^0$) for ECT dissolution in various “PEG-400 + water” mixtures and pure solvents were found as positive values in the range of 11.75 to 14.35 kJ mol⁻¹, indicating “endothermic dissolution” of ECT in all cosolvent mixtures including pure water and pure PEG-400 [6,7]. The “ $\Delta_{\text{sol}}H^0$ values” of ECT were found to decrease with increase in the m value of PEG-400 in “PEG-400 + water” mixtures and solubility of ECT. Hence, the maximum “ $\Delta_{\text{sol}}H^0$ value” was found in pure water (14.35 kJ mol⁻¹), while, the minimum one was recorded in pure PEG-400 (11.75 kJ mol⁻¹).

Table 4. Apparent thermodynamic parameters [apparent standard enthalpy ($\Delta_{\text{sol}}H^0$), apparent standard Gibbs energy ($\Delta_{\text{sol}}G^0$) and apparent standard entropy ($\Delta_{\text{sol}}S^0$)] and R^2 values for ECT dissolution in various “PEG-400 + water” mixtures (m)^b.

m	$\Delta_{\text{sol}}H^0/\text{kJ mol}^{-1}$	$\Delta_{\text{sol}}G^0/\text{kJ mol}^{-1}$	$\Delta_{\text{sol}}S^0/\text{J mol}^{-1} \text{K}^{-1}$	R^2
0.0	14.35	11.91	7.94	0.9995
0.1	13.80	11.31	8.05	0.9956
0.2	13.72	10.67	9.90	0.9980
0.3	13.43	9.98	11.21	0.9975
0.4	13.35	9.25	13.30	0.9988
0.5	13.12	8.59	14.68	0.9992
0.6	12.79	7.94	15.75	0.9980
0.7	12.44	7.28	16.73	0.9984
0.8	12.27	6.65	18.24	0.9989
0.9	11.38	5.99	17.51	0.9976
1.0	11.75	5.32	20.86	0.9967

^b Mean relative uncertainties are $u(\Delta_{\text{sol}}H^0) = 0.07$, $u(\Delta_{\text{sol}}G^0) = 0.25$ and $u(\Delta_{\text{sol}}S^0) = 0.30$.

The values of apparent standard Gibbs free energies ($\Delta_{\text{sol}}G^0$) for ECT dissolution in various “PEG-400 + water” mixtures were also recorded as positive values in the range of 5.32 to 11.91 kJ mol⁻¹ (Table 4). The “ $\Delta_{\text{sol}}G^0$ values” for ECT dissolution were also found decreased with increase in m value of PEG-400 in “PEG-400 + water” mixtures and solubility values of ECT. The maximum and minimum “ $\Delta_{\text{sol}}G^0$ values” for ECT dissolution were observed in pure water (11.91 kJ mol⁻¹) and pure PEG-400 (5.32 kJ mol⁻¹), respectively.

The values of apparent standard entropies ($\Delta_{\text{sol}}S^0$) for ECT dissolution in various “PEG-400 + water” mixtures were also obtained as positive values in the range of 9.94 to 20.86 J mol⁻¹ K⁻¹,

indicating “entropy-driven dissolution” of ECT in all “PEG-400 + water” combinations including pure water and pure PEG-400 [7]. The mean relative uncertainties in “ $\Delta_{\text{sol}}H^0$, $\Delta_{\text{sol}}G^0$ and $\Delta_{\text{sol}}S^0$ ” were found as 0.07, 0.25 and 0.30, respectively. Based on these results, the overall dissolution of ECT was found as an “endothermic and entropy-driven” in all “PEG-400 + water” mixtures and pure solvents [6,7].

2.6. Solvation Analysis of ECT

The solvation behavior of ECT in various “PEG-400 + water” mixtures was studied using “enthalpy–entropy compensation analysis” and results are summarized in Figure 4. It was found that ECT in all “PEG-400 + water” mixtures and pure solvents expressed a non-linear “ $\Delta_{\text{sol}}H^0$ vs. $\Delta_{\text{sol}}G^0$ ” curve with a positive slope value of 1.40. Based on this observation, the “driving mechanism” for ECT solvation was proposed as an “enthalpy-driven” in all “PEG-400 + water” mixtures and pure solvents. This observation was probably due to higher solvation of ECT in pure PEG-400 molecules compared with pure water molecules [7]. The solvation behavior of ECT in various “PEG-400 + water” mixtures recorded in this study was in accordance with those proposed for the solvation mechanism of ferulic acid, 4-(4-ethoxyphenyl)-5-(3,4,5-trimethoxybenzoyl)-3,4-dihydropyrimidine-2(1*H*)-one, lornoxicam, hydrazide derivative, isatin, paracetamol and sulfadiazine in various “PEG-400 + water” mixtures [7, 11,12,31–34].

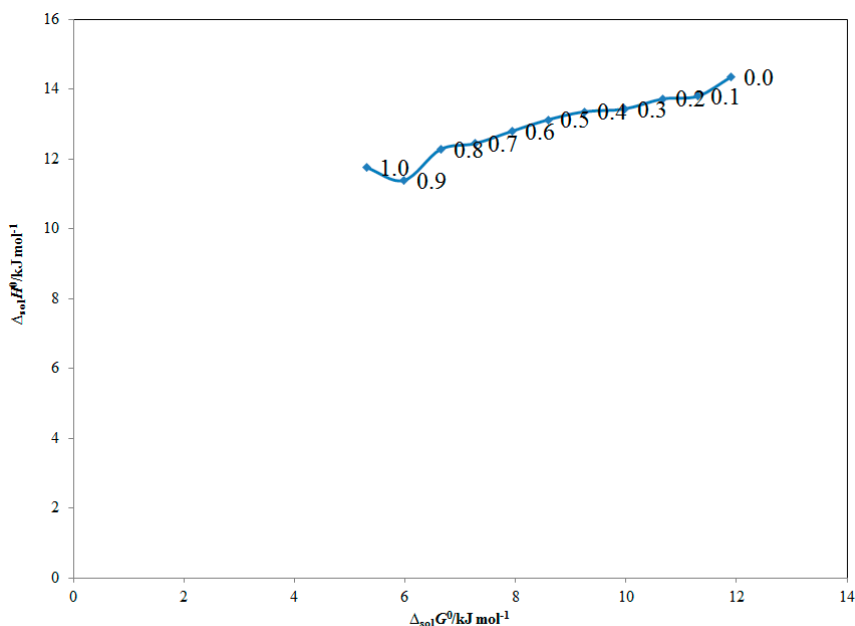


Figure 4. Apparent standard enthalpy ($\Delta_{\text{sol}}H^0$) vs. apparent standard Gibbs energy ($\Delta_{\text{sol}}G^0$) “enthalpy–entropy compensation” graph for ECT in different “PEG-400 + water” combinations at T_{hm} value of 308 K.

2.7. Computation Modeling

The experimental solubility data of ECT was correlated and validated using five different computational models including “Van’t Hoff, Apelblat, Yalkowsky-Roseman, Jouyban-Acree and Jouyban-Acree-Van’t Hoff models”. The “Van’t Hoff model solubility ($x^{\text{Van't}}$)” of ECT was calculated by applying Equation (11) and the x_e value of ECT was correlated with its $x^{\text{Van't}}$ value using “root mean square deviation (RMSD) and determination coefficient (R^2)” values. The resulting data of “Van’t Hoff model” for ECT in various “PEG-400 + water” mixtures, including pure water and pure PEG-400, are summarized in Table 5. RMSDs for ECT in various “PEG-400 + water” mixtures, including pure water and pure PEG-400, were computed as 0.42% to 0.91% with an overall RMSD value of 0.73%. The R^2 values for “Van’t Hoff model” were obtained as 0.9955 to 0.9995.

Table 5. The parameters of “Van’t Hoff model (*a* and *b*)” along with R^2 and % root mean square deviations (% *RMSDs*) for ECT in various “PEG-400 + water” combinations (*m*)^c.

<i>m</i>	<i>a</i>	<i>b</i>	R^2	<i>RMSD</i> (%)	Overall <i>RMSD</i> (%)
0.0	0.94	−1724.70	0.9995	0.78	
0.1	0.96	−1657.60	0.9955	0.89	
0.2	1.18	−1648.50	0.9979	0.79	
0.3	1.34	−1614.10	0.9976	0.55	
0.4	1.59	−1604.20	0.9988	0.53	
0.5	1.75	−1575.90	0.9991	0.91	0.73
0.6	1.88	−1537.10	0.9981	0.90	
0.7	2.00	−1494.50	0.9984	0.79	
0.8	2.18	−1474.90	0.9989	0.78	
0.9	2.10	−1368.10	0.9977	0.42	
1.0	2.50	−1412.30	0.9967	0.69	

^c The average relative uncertainties are $u(a) = 0.30$ and $u(b) = 0.07$.

The “Apelblat model solubility (x^{Ap1})” of ECT was calculated by applying Equation (12) and the x_e value of ECT was correlated with its x^{Ap1} value in using “*RMSD* and R^2 ” values. The results of the “Apelblat model” for ECT in various “PEG-400 + water” mixtures and pure solvents are summarized in Table 6.

Table 6. The parameters of “Apelblat model (*A*, *B* and *C*)” along with R^2 and % *RMSDs* for ECT in various “PEG-400 + water” combinations (*m*)^d.

<i>m</i>	<i>A</i>	<i>B</i>	<i>C</i>	R^2	<i>RMSD</i> (%)	Overall <i>RMSD</i> (%)
0.0	−81.15	2029.00	12.20	0.9998	0.19	
0.1	−234.90	9119.87	35.05	0.9994	0.67	
0.2	−82.67	2184.81	12.46	0.9985	0.57	
0.3	27.91	−2824.59	−3.95	0.9974	0.62	
0.4	−109.75	3485.30	16.54	0.9996	0.28	
0.5	−97.65	2968.30	14.77	0.9998	0.19	0.46
0.6	−84.07	2392.73	12.77	0.9985	0.48	
0.7	−93.52	2872.33	14.19	0.9990	0.46	
0.8	−61.36	1430.99	9.44	0.9991	0.36	
0.9	24.32	−2380.72	−3.30	0.9975	0.60	
1.0	−56.49	1285.38	8.76	0.9968	0.74	

^d The average relative uncertainties are $u(A) = 0.92$, $u(B) = 1.54$ and $u(C) = 0.90$.

The *RMSD* values for ECT in various “PEG-400 + water” mixtures and pure solvents were estimated as 0.19% to 0.74% with an overall *RMSD* of 0.46%. The R^2 values for the “Apelblat model” were recorded as 0.9968 to 0.9998. Graphical correlation between x_e and x^{Ap1} values of ECT are summarized in Figure 5, indicating good graphical correlation of x_e values of ECT with the “Apelblat model”.

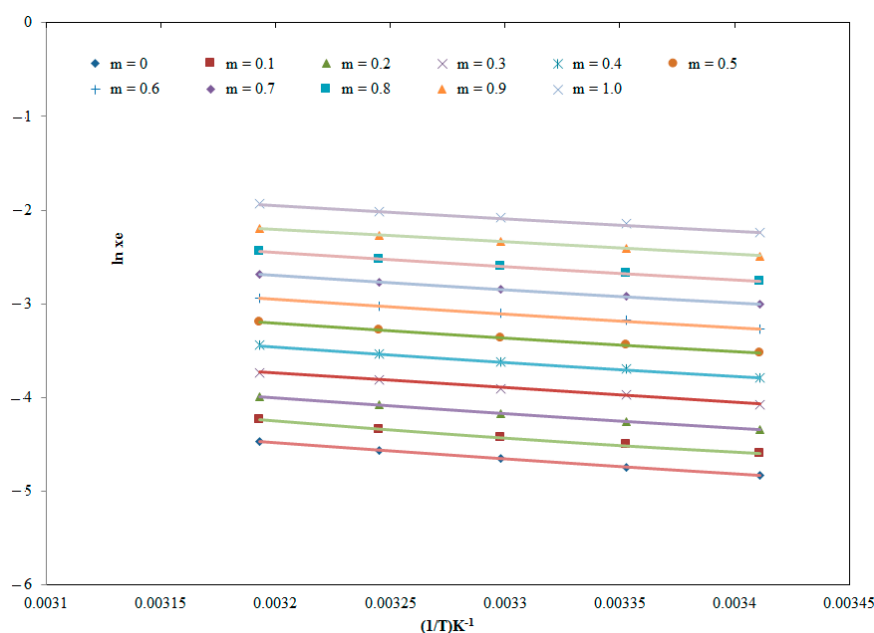


Figure 5. Graphical correlation of logarithmic solubilities of ECT with the “Apelblat model” in various “PEG-400 + water” combinations at “ $T = 298.2$ to 318.2 K” (solid lines indicate the “Apelblat solubilities” of ECT and symbols indicate the experimental solubilities of ECT).

The “logarithmic solubility of Yalkowsky-Roseman model ($\log x^{\text{Yal}}$)” of ECT was calculated by applying Equation (13) and the correlation between x_e and x^{Yal} values of ECT was performed in terms of *RMSD* values.

Resulting data of the “Yalkowsky-Roseman model” for ECT in various “PEG-400 + water” mixtures, including pure water and pure PEG-400, are summarized in Table 7. The *RMSDs* for the “Yalkowsky-Roseman model” were found as 0.44% to 2.98% with an overall *RMSD* value of 1.33%.

Table 7. $\log x^{\text{Yal}}$ values of ECT obtained by the “Yalkowsky-Roseman” model in various “PEG-400 + water” combinations (m) at “ $T = 298.2$ to 318.2 K”.

m	$\log x^{\text{Yal}}$					<i>RMSD</i> (%)	Overall <i>RMSD</i> (%)
	298.2 K	303.2 K	308.2 K	313.2 K	318.2 K		
0.1	-1.98	-1.94	-1.90	-1.86	-1.82	2.86	
0.2	-1.87	-1.83	-1.79	-1.75	-1.71	2.98	
0.3	-1.76	-1.72	-1.68	-1.64	-1.60	1.92	
0.4	-1.64	-1.60	-1.57	-1.53	-1.49	0.81	
0.5	-1.53	-1.49	-1.46	-1.42	-1.38	0.87	1.33
0.6	-1.42	-1.38	-1.34	-1.31	-1.27	0.78	
0.7	-1.30	-1.27	-1.23	-1.20	-1.16	0.79	
0.8	-1.19	-1.15	-1.12	-1.09	-1.05	0.57	
0.9	-1.08	-1.04	-1.01	-0.98	-0.94	0.44	

Resulting data of the “Jouyban-Acree model” (Equation (14)) and the “Jouyban-Acree-Van’t Hoff model” (Equation (15)) for ECT in “PEG-400 + water” mixtures are summarized in Table 8. An overall *RMSD* for the “Jouyban-Acree model” was found as 0.42%. While, an overall *RMSD* for the “Jouyban-Acree-Van’t Hoff model” was found as 0.61%. In general, all computational models represented good correlation based on *RMSD* values, but the “Jouyban-Acree” model was found as the most accurate and precise because it utilized the least number of model parameters compared with other models.

Table 8. The parameters of the “Jouyban-Acree” and the “Jouyban-Acree-van’t Hoff” models for ECT in “PEG-400 + water” mixtures.

System	Jouyban-Acree	Jouyban-Acree-van’t Hoff
PEG-400 + water	J_i 23.41	A_1 2.50 B_1 -1412.30 A_2 0.94 B_2 -1724.70
RMSD (%)	0.42	J_i 21.32 0.61

3. Materials and Methods

3.1. Materials

ECT was procured from “Sigma-Aldrich (St. Louis, MO, USA). PEG-400 (average molar mass = 400 g mol⁻¹ and polydispersity index = 1.04) was obtained from Fluka Chemica (Busch, Switzerland). The chromatography-grade water was collected from “Milli-Q water purification unit” in the laboratory. The list of materials along with their detailed properties are summarized in Table 9.

Table 9. List of materials and their properties.

Material	Molecular Formula	Molar Mass (g mol ⁻¹)	CAS Registry No.	Purification Method	Mass Fraction Purity	Analysis Method	Source
ECT	C ₈ H ₁₀ FN ₃ O ₃ S	247.24	143491-54-7	None	>0.98	HPLC	Sigma-Aldrich
PEG-400	H(OCH ₂ CH ₂) _n OH	400	25322-68-3	None	>0.99	HPLC	Fluka Chemica
Water	H ₂ O	18.07	7732-18-5	None	-	-	Milli-Q

The purity and method of analysis was provided by the supplier of each material.

3.2. Solid Phase Characterization of ECT

The solid phase characterization of ECT in its pure form and equilibrated sample was performed by XRD analysis. The XRD analysis of ECT in pure and equilibrated samples was performed by “Ultima IV Diffractometer (Rigaku Inc. Tokyo, Japan)”. The diffraction angle (2θ) range for this analysis was set at 3°–120° with a scan speed of 1.0° min⁻¹ for both samples. The rest of the operation and condition was similar to those reported in our previous article [29].

3.3. Determination of ECT Solubility in Various “PEG-400 + Water” Mixtures

The solubility of ECT in various “PEG-400 + water” mixtures and mono solvents was determined at “ $T = 298.2$ to 318.2 K” and “ $p = 0.1$ MPa” using a reported isothermal method [35]. Before determining the solubility of ECT, the reliability of experimental method was verified by determining the solubility of isatin in pure water at $T = 298.2$ and $T = 318.2$ K. The solubility of isatin in pure water could be compared with existing literature values [11]. The excess amount of ECT was taken in fixed amounts of various “PEG-400 + water” mixtures and mono solvents. Each analysis was repeated for three times ($n = 3$). The obtained dispersions were vortex mixed for about 5 min and transferred to “WiseBath® WSB Shaking Water Bath (Model WSB-18/30/-45, Daihan Scientific Co. Ltd., Seoul, Korea)” for equilibrium/saturation. The speed and equilibrium time of shaker were set at 100 rpm and 72 h, respectively [7]. The temperature of measurement was changed as mentioned above. The uncertainty in the temperature of “WiseBath® WSB Shaking Water Bath” was computed as ± 0.10 K. After 72 h, each mixture was withdrawn carefully and ECT particles were allowed to settle overnight [7,8]. Then, the supernatant of each sample was taken, diluted (wherever applicable) and subjected for the analysis of ECT concentration by high-performance liquid chromatography method at the wavelength of 254

nm. The binary mixture of “methanol:ethanol (1:1 % v/v)” was used as a mobile phase for this analysis. The x_e values of ECT were calculated using the following Equations [32,33]:

$$x_e = \frac{m_1/M_1}{m_1/M_1 + m_2/M_2} \quad (1)$$

$$x_e = \frac{m_1/M_1}{m_1/M_1 + m_2/M_2 + m_3/M_3} \quad (2)$$

where m_1 = mass of ECT; m_2 = mass of PEG-400; m_3 = mass of water; M_1 = molar mass of ECT; M_2 = molar mass of PEG-400 and M_3 = molar mass of water.

3.4. HSPs of ECT and Various “PEG-400 + Water” Mixtures

The HSP of solute is associated with its solubility in pure solvent or cosolvent–water mixtures. If the HSP of solute is closed with that of pure solvent or cosolvent–water mixtures, the solubility of solute will be higher in that pure solvent or cosolvent–water mixture [36]. Hence, HSP for ECT, pure PEG-400, pure water and various “PEG-400 + water” mixtures free of ECT were computed in this study. The δ values for ECT, pure PEG-400 and pure water were computed using the following Equation [37–39]:

$$\delta^2 = \delta_d^2 + \delta_p^2 + \delta_h^2 \quad (3)$$

where “ δ = total HSP; δ_d = dispersion HSP; δ_p = polar HSP and δ_h = hydrogen-bonded HSP”. The values of HSP for ECT and mono solvents were computed using “HSPiP software (version 4.1.07, Louisville, KY, USA)” by putting the smiles of ECT and mono solvents into the software [38]. The HSP for various “PEG-400 + water” mixtures free of ECT (δ_{mix}) was computed using the following Equation [40,41]:

$$\delta_{\text{mix}} = \alpha \delta_1 + (1 - \alpha) \delta_2 \quad (4)$$

where α = volume fraction of PEG-400 in “PEG-400 + water” mixtures; δ_1 = HSP of pure PEG-400 and δ_2 = HSP of pure water.

3.5. Ideal Solubilities and Activity Coefficients

The x^{idl} values of ECT at five different temperatures were computed using the following Equation [42]:

$$\ln x^{\text{idl}} = \frac{-\Delta H_{\text{fus}}(T_{\text{fus}} - T)}{RT_{\text{fus}}T} + \left(\frac{\Delta C_p}{R} \right) \left[\frac{T_{\text{fus}} - T}{T} + \ln \left(\frac{T}{T_{\text{fus}}} \right) \right] \quad (5)$$

where T = absolute temperature; T_{fus} = fusion temperature of ECT; R = universal gas constant; ΔH_{fus} = molar fusion enthalpy of ECT and ΔC_p = difference in the molar heat capacity of solid state with that of liquid state of ECT [42,43]. The quantitative values of “ T_{fus} , ΔH_{fus} and ΔC_p ” for ECT were computed as 427.80 K, 32.37 kJ mol⁻¹ and 75.66 J mol⁻¹ K⁻¹, respectively using thermal analysis. Now, the x^{idl} values for ECT were computed by applying Equation (5).

The γ_i values for ECT in various “PEG-400 + water” mixtures were computed using the following equation [42,44]:

$$\gamma_i = \frac{x^{\text{idl}}}{x_e} \quad (6)$$

Using the quantitative values of γ_i , the molecular interactions between solute and the solvents were computed.

3.6. Thermodynamic Behavior of ECT

The dissolution behavior of ECT in various “PEG-400 + water” mixtures and mono solvents was evaluated by applying “apparent thermodynamic analysis” using “Van’t Hoff and Gibbs Equations”. The “van’t Hoff Equation” was used to found out apparent thermodynamic parameters of ECT in

various “PEG-400 + water” mixtures, which was obtained at mean harmonic temperature (T_{hm}) of 308 K within the temperature range of “ $T = 298.2$ to 318.2 K”, and is expressed using the following Equation [42,45]:

$$\left(\frac{\partial \ln x_e}{\partial \left(\frac{1}{T} - \frac{1}{T_{hm}} \right)} \right)_P = -\frac{\Delta_{sol}H^0}{R} \quad (7)$$

By plotting $\ln x_e$ values of ECT against $\frac{1}{T} - \frac{1}{T_{hm}}$, the $\Delta_{sol}H^0$ and $\Delta_{sol}G^0$ values for ECT dissolution were computed from the slope and intercept, respectively, using the following Equations [46]:

$$\Delta_{sol}H^0 = -R \left(\frac{\partial \ln x_e}{\partial \left(\frac{1}{T} - \frac{1}{T_{hm}} \right)} \right)_P \quad (8)$$

$$\Delta_{sol}G^0 = -RT_{hm} \times \text{intercept} \quad (9)$$

Finally, the $\Delta_{sol}S^0$ values for ECT dissolution in various “PEG-400 + water” mixtures and mono solvents were computed using the following Gibbs Equation [42,45,46]:

$$\Delta_{sol}S^0 = \frac{\Delta_{sol}H^0 - \Delta_{sol}G^0}{T_{hm}} \quad (10)$$

3.7. Enthalpy–Entropy Compensation Analysis

The solvation analysis of ECT in various “PEG-400 + water” mixtures and mono solvents was computed by applying “enthalpy–entropy compensation analysis” [7,45]. This analysis was conducted by plotting the weighted plots of “ $\Delta_{sol}H^0$ vs. $\Delta_{sol}G^0$ ” at $T_{hm} = 308$ K [7].

3.8. Computational Models

In this study, the x_e values of ECT were validated and correlated with five different computational models such as “Van’t Hoff, Apelblat, Yalkowsky-Roseman, Jouyban-Acree and Jouyban-Acree-Van’t Hoff” models [31,47–52].

The $x^{\text{Van't}}$ values of ECT in various “PEG-400 + water” combinations including pure water and pure PEG-400 were calculated by applying the following Equation [31]:

$$\ln x^{\text{Van't}} = a + \frac{b}{T} \quad (11)$$

where “ a and b = model parameters of Equation (11)” which were computed by drawing the plots between $\ln x_e$ values of ECT and $1/T$.

The x^{Apl} values of ECT in various “PEG-400 + water” mixtures including pure water and pure PEG-400 were obtained by applying the following Equation [47,48]:

$$\ln x^{\text{Apl}} = A + \frac{B}{T} + C \ln(T) \quad (12)$$

where “ A , B and C = model parameters Equation (12)” which were computed by applying “nonlinear multivariate regression analysis” of x_e values of ECT summarized in Table 1 [31].

The $\log x^{\text{Yal}}$ values for ECT in various “PEG-400 + water” combinations including pure water and pure PEG-400 were estimated by applying the following Equation [49]:

$$\text{Log} x^{\text{Yal}} = m_1 \log x_1 + m_2 \log x_2 \quad (13)$$

where x_1 = mole fraction solubility of ECT in pure PEG-400; x_2 = mole fraction solubility of ECT in pure water; m_1 = mass fraction of pure PEG-400 and m_2 = mass fraction of pure water in the absence of ECT.

The “Jouyban-Acree model solubility ($x_{m,T}$)” of ECT in “PEG-400 + water” mixtures was estimated by applying the following Equation [31,50–52]:

$$\ln x_{m,T} = m_1 \ln x_1 + m_2 \ln x_2 + \left[m_1 m_2 \sum_{i=0}^2 \frac{J_i}{T} (m_1 - m_2)^i \right] \quad (14)$$

where “ J_i = model parameter of Equation (14)” and it was computed from “no-intercept regression analysis” [31,53].

The “Jouyban-Acree-van’t Hoff” solubility of ECT in “PEG-400 + water” mixtures was estimated by applying the following Equation [31,54]:

$$\ln x_{m,T} = m_1 \left(A_1 + \frac{B_1}{T} \right) + m_2 \left(A_2 + \frac{B_2}{T} \right) + \left[\frac{m_1 m_2}{T} \sum_{i=0}^2 J_i (m_1 - m_2)^i \right] \quad (15)$$

where “ A_1, B_1, A_2, B_2 and J_i = model parameters of Equation (15)”.

3.9. Statistical Analysis

Statistical analysis was done by applying the “Kruskal–Wallis test” followed by the Denn’s test using “GraphpadInstat software (San Diego, CA, USA)”. The $p < 0.05$ was considered as significant value.

4. Conclusions

This study aimed to find out solubility, HSPs and apparent thermodynamic parameters of ECT in various “PEG-400 + water” mixtures and pure solvents at “ $T = 298.2$ to 318.2 K” and “ $p = 0.1$ MPa”. Experimental solubilities of ECT were correlated well by “Van’t Hoff, Apelblat, Yalkowsky-Roseman, Jouyban-Acree and Jouyban-Acree-Van’t Hoff” models. In general, all computational models performed well in terms of *RMSD* values, but the Jouyban-Acree model was found as the most accurate and precise as it utilized the least number of model parameters. The solubilities of ECT were found to enhance with the raise in temperature and the increase in the m value of PEG-400 in all “PEG-400 + water” mixtures and pure solvents. The solubility results were in accordance with their HSPs and polarity. The data of activity coefficients indicated maximum molecular interactions in ECT-PEG-400 compared with ECT-water. “Apparent thermodynamic analysis” showed an “endothermic and entropy-driven” dissolution of ECT in various “PEG-400 + water” mixtures and pure solvents. “Enthalpy–entropy compensation” analysis indicated that the solvation behavior of ECT was “enthalpy-driven” in all “PEG-400 + water” mixtures and mono solvents.

Author Contributions: Conceptualization, supervision—F.S.; methodology—N.H., I.A.A. and S.A.; validation—N.H. and S.A.; writing—original draft—F.S. and S.A.; writing—review and editing—N.H., I.A.A. and S.A.; software—F.S. and S.A. All authors have read and agreed to the published version of the manuscript.

Funding: This research was funded by the Researchers Supporting Project (number RSP-2019/146) at King Saud University, Riyadh, Saudi Arabia and APC was also supported by RSP.

Acknowledgments: Authors are thankful to the Researchers Supporting Project (number RSP-2019/146) at King Saud University, Riyadh, Saudi Arabia.

Conflicts of Interest: The authors report no conflicts of interest associated with this manuscript.

References

1. U.S. Department of Health and Human Services, Food and Drug Administration (FDA), Center for Evaluation and Research (CDER). *Emtriva*® (*Emtricitabine*) Capsules and Oral Solution. *Guidance for Industry; Draft Guidance*; Food and Drug Administration (FDA): Washington, DC, USA, 2018.

2. Ploger, G.F.; Hofsass, M.A.; Dressman, J.B. Solubility determination of active pharmaceutical ingredients which have been recently added to the list of essential medicines in the context of the biopharmaceutics classification system-biowaiver. *J. Pharm. Sci.* **2018**, *107*, 1478–1488. [[CrossRef](#)] [[PubMed](#)]
3. Nathan, B.; Bayley, J.; Waters, L.; Post, F.A. Cobicistat: A novel pharmacoenhancer for co-formulation with HIV protease and integrase inhibitors. *Infect. Dis. Ther.* **2013**, *2*, 111–122. [[CrossRef](#)] [[PubMed](#)]
4. Siyawamwaya, M.; Toit, L.C.D.; Kumar, P.; Choonara, Y.E.; Kodiah, P.P.P.D.; Pillay, V. 3D printed, controlled release, tritherapeutic matrix tablet matrix for advanced anti-HIV-I drug delivery. *Eur. J. Pharm. Biopharm.* **2019**, *138*, 99–110. [[CrossRef](#)] [[PubMed](#)]
5. Singh, G.; Pai, R.S. Pharmacokinetics and in vivo biodistribution of optimized PLGA nanoparticulate drug delivery system for controlled release of emtricitabine. *Drug Deliv.* **2014**, *21*, 627–635. [[CrossRef](#)] [[PubMed](#)]
6. Shakeel, F.; Alshehri, S.; Imran, M.; Haq, N.; Alanazi, A.; Anwer, M.K. Experimental and computational approaches for solubility measurement of pyridazinone derivative in binary (DMSO + water) systems. *Molecules* **2020**, *25*, 171. [[CrossRef](#)]
7. Shakeel, F.; Haq, N.; Siddiqui, N.A. Thermodynamic solubility and solvation behavior of ferulic acid in different (PEG-400 + water) binary solvent mixtures. *Drug Dev. Ind. Pharm.* **2019**, *45*, 1468–1476. [[CrossRef](#)]
8. Shakeel, F.; Alshehri, S.; Haq, N.; Elzayat, E.; Ibrahim, M.; Altamimi, M.A.; Mohsin, K.; Alanazi, F.K.; Alsarra, I.A. Solubility determination and thermodynamic data of apigenin in binary (Transcutol[®] + water) mixtures. *Ind. Crops Prod.* **2018**, *116*, 56–63. [[CrossRef](#)]
9. Cardenas, Z.J.; Jimenez, D.M.; Martinez, F. Solubility and solution thermodynamics of meloxicam in polyethylene glycol 400 + water mixtures. *J. Mol. Liq.* **2015**, *211*, 233–238. [[CrossRef](#)]
10. Shakeel, F.; Haq, N.; Alanazi, F.K.; Alsarra, I.A. Solubility and thermodynamics of tenoxicam in (PEG-400 + water) binary solvent systems at different temperatures. *J. Mol. Liq.* **2016**, *213*, 221–227. [[CrossRef](#)]
11. Shakeel, F.; Haq, N.; Alanazi, F.K.; Alsarra, I.A. Thermodynamics of solubility of isatin in (PEG 400 + water) mixed solvent systems at T = (298.15 to 338.15) K. *J. Chem. Thermodyn.* **2015**, *82*, 156–160. [[CrossRef](#)]
12. Jimenez, D.M.; Cardenas, Z.J.; Martinez, F. Solubility and solution thermodynamics of sulfadiazine in polyethylene glycol 400 + water mixtures. *J. Mol. Liq.* **2016**, *216*, 239–245. [[CrossRef](#)]
13. Soltanpour, S.; Gharagozlu, A. Piroxicam solubility in binary and ternary solvents of polyethylene glycols 200 or 400 with ethanol and water at 298.2 K: Experimental data report and modeling. *J. Sol. Chem.* **2015**, *44*, 1407–1423. [[CrossRef](#)]
14. Soltanpour, S.; Shekarriz, A.H. Naproxen solubility in binary and ternary solvents of polyethylene glycols 200, 400 or 600 with ethanol and water at 298.2 K: Experimental data report and modeling. *Phys. Chem. Liq.* **2015**, *53*, 748–762. [[CrossRef](#)]
15. Imran, M. Solubility and thermodynamics of 6-phenyl-4,5-dihydropyridazin-3(2H)-one in various (PEG 400 + water) mixtures. *Z. Phys. Chem.* **2019**, *233*, 273–287. [[CrossRef](#)]
16. Jouyban, A.; Shakeel, F.; Bhat, M.A.; Acree, W.E., Jr.; Martinez, F. Preferential solvation of 4-(4-ethoxyphenyl)-5-(3,4,5-trimethoxybenzoyl)-3,4-dihydropyrimidin-2(1H)-one in {PEG 400 (1) + water (2)} mixtures. *Phys. Chem. Liq.* **2020**. [[CrossRef](#)]
17. Mohammadian, E.; Rahimpour, E.; Martinez, F.; Jouyban, A. Budesonide solubility in polyethylene glycol 400 + water at different temperatures: Experimental measurement and mathematical modelling. *J. Mol. Liq.* **2019**, *274*, 418–425. [[CrossRef](#)]
18. Dadmand, S.; Kamari, F.; Acree, W.E., Jr.; Jouyban, A. Solubility prediction of drugs in binary solvent mixtures at various temperatures using a minimum number of experimental data points. *AAPS PharmSciTech.* **2019**, *20*, E10. [[CrossRef](#)]
19. Srilatha, U.; Rama Krishna, M.; Vasavi Reddy, D.; Devireddy, S.R. Formulation and evaluation of emtricitabine and tinofovir disoproxil fumarate film coated tablets. *Int. J. Res. Pharm. Chem.* **2015**, *5*, 116–125.
20. Clark, M.R.; Peet, M.M.; Davis, S.; Doncel, G.F.; Friend, D.R. Evaluation of rapidly disintegrating vaginal tablets of tinofovir, emtricitabine and their combination for HIV-1 prevention. *Pharmaceutics* **2014**, *6*, 616–631. [[CrossRef](#)]
21. Manikandan, M.; Kannan, K.; Selvamuthukumar, S.; Manavalan, R. Formulation development and evaluation of emtricitabine and tinofovir disoproxil fumarate tablets. *Int. J. Drug. Dev. Res.* **2012**, *4*, 247–256.
22. Forbes, C.J.; McCoy, C.F.; Murphy, D.J.; Woolfson, A.D.; Moore, J.P.; Evans, A.; Shattock, R.J.; Malcolm, R.K. Modified silicone elastomer vaginal gels for sustained release of antiretroviral HIV microbicides. *J. Pharm. Sci.* **2014**, *103*, 1422–1432. [[CrossRef](#)] [[PubMed](#)]

23. Faria, M.J.; Machado, R.; Ribeiro, A.; Goncalves, H.; Elisabete, M.; Oliveira, C.D.R.; Viseu, T.; Neves, J.D.; Lucio, M. Rational development of liposomal hydrogels: A strategy for topical vaginal antiretroviral drug delivery in the context of HIV prevention. *Pharmaceutics* **2019**, *11*, 485. [[CrossRef](#)] [[PubMed](#)]
24. Fathima, A.; Hari, B.N.V.; Devi, D.R. Development of microparticulate sustained release dosage form of emtricitabine: An anti-HIV drug. *Asian J. Chem.* **2014**, *26*, 2604–2610. [[CrossRef](#)]
25. Ibrahim, M.; Bade, A.N.; Lin, Z.; Soni, D.; Wojtkiewicz, M.; Shetty, B.L.D.; Gautam, N.; McMillan, J.M.; Alnouti, Y.; Edagwa, B.J.; et al. Synthesis and characterization of a long-acting emtricitabine prodrug nanoformulation. *Int. J. Nanomed.* **2019**, *14*, 6231–6247. [[CrossRef](#)]
26. Soni, D.; Bade, A.N.; Gautam, N.; Herskovitz, J.; Ibrahim, I.M.; Smith, N.; Wojtkiewicz, M.S.; Shetty, B.L.D.; Alnouti, Y.; McMillan, J.; et al. Synthesis of a long-acting nanoformulated emtricitabine ProTide. *Biomaterials* **2019**, *222*, E119441. [[CrossRef](#)]
27. Mandal, S.; Belshan, M.; Holec, A.; Zhou, Y.; Destache, C.J. An enhanced emtricitabine-loaded long-acting nanoformulation for prevention or treatment of HIV infection. *Antimic. Agents Chemother.* **2017**, *61*, E01475-16. [[CrossRef](#)]
28. Mandal, S.; Kang, G.; Prathipati, P.K.; Fan, W.; Li, Q.; Destache, C.J. Long-acting parenteral combination antiretroviral loaded nano-drug delivery system to treat chronic HIV-1 infection: A humanized mouse model study. *Antiviral Res.* **2018**, *156*, 85–91. [[CrossRef](#)]
29. Shakeel, F.; Imran, M.; Haq, N.; Alshehri, S.; Anwer, M.K. Synthesis, characterization and solubility determination of 6-phenyl-pyridazin-3(2H)-one in different pharmaceutical solvents. *Molecules* **2019**, *24*, 3404. [[CrossRef](#)]
30. Alshehri, S.; Imam, S.S.; Altamimi, M.A.; Hussain, A.; Shakeel, F.; Elzayat, E.; Mohsin, K.; Ibrahim, M.; Alanazi, F. Enhanced dissolution of luteolin by solid dispersion prepared by different methods: Physicochemical characterization and antioxidant activity. *ACS Omega* **2020**. [[CrossRef](#)]
31. Shakeel, F.; Bhat, M.A.; Haq, N.; Fatih-Azarbayjani, A.; Jouyban, A. Solubility and thermodynamic parameters of a novel anti-cancer drug (DHP-5) in polyethylene glycol 400 + water mixtures. *J. Mol. Liq.* **2017**, *229*, 241–245. [[CrossRef](#)]
32. Shakeel, F.; Haq, N.; Alanazi, F.K.; Alsarra, I.A. Solubility and thermodynamic function of lornoxicam in (PEG-400 + water) mixtures at different temperatures. *J. Mol. Liq.* **2016**, *219*, 439–443. [[CrossRef](#)]
33. Shakeel, F.; Haq, N.; Radwan, A.A.; Alanazi, F.K.; Alsarra, I.A. Solubility and solvation behavior of N'-(1-(N-(methyl) benzylaminomethyl)-2-oxoindolin-3-ylidene)-2-(benzyloxy) benzohydrazide in (PEG 400 + water) mixtures. *J. Mol. Liq.* **2016**, *221*, 1225–1230. [[CrossRef](#)]
34. Ahumada, E.A.; Delgado, D.R.; Martínez, F. Solution thermodynamics of acetaminophen in some polyethylene glycol 400 + water mixtures. *Fluid Phase Equilib.* **2012**, *332*, 120–127. [[CrossRef](#)]
35. Higuchi, T.; Connors, K.A. Phase-solubility techniques. *Adv. Anal. Chem. Inst.* **1965**, *4*, 117–122.
36. Zhu, Q.N.; Wang, Q.; Hu, Y.B.; Abliz, X. Practical determination of the solubility parameters of 1-alkyl-3-methylimidazolium bromide ([CnC1im]Br, n = 5, 6, 7, 8) ionic liquids by inverse gas chromatography and the Hansen solubility parameter. *Molecules* **2019**, *24*, 1346. [[CrossRef](#)] [[PubMed](#)]
37. Alanazi, A.; Alshehri, S.; Altamimi, M.; Shakeel, F. Solubility determination and three dimensional Hansen solubility parameters of gefitinib in different organic solvents: Experimental and computational approaches. *J. Mol. Liq.* **2020**, *299*, E112211. [[CrossRef](#)]
38. Kalam, M.A.; Alshamsan, A.; Alkholief, M.; Alsarra, I.A.; Ali, R.; Haq, N.; Anwer, M.K.; Shakeel, F. Solubility measurement and various solubility parameters of glipizide in different neat solvents. *ACS Omega* **2020**, *5*, 1708–1716. [[CrossRef](#)]
39. Anwer, M.K.; Muqtader, M.; Iqbal, M.; Ali, R.; Almutairy, B.K.; Alshetaili, A.; Alshahrani, S.M.; Aldawsari, M.F.; Alalaiwe, A.; Shakeel, F. Estimating the solubility, solution thermodynamics, and molecular interactions of aliskiren hemifumarate in alkyl imidazolium based ionic liquids. *Molecules* **2019**, *24*, 2807. [[CrossRef](#)]
40. Wan, Y.; He, H.; Huang, Z.; Zhang, P.; Sha, J.; Li, T.; Ren, B. Solubility, thermodynamic modeling and Hansen solubility parameter of 5-norbornene-2,3-dicarboximide in three binary solvents (methanol, ethanol, ethyl acetate + DMF) from 278.15 K to 323.15 K. *J. Mol. Liq.* **2020**, *300*, E112097. [[CrossRef](#)]
41. Shakeel, F.; Haq, N.; Alanazi, F.K.; Alanazi, S.A.; Alsarra, I.A. Solubility of sinapic acid in various (Carbitol + water) systems: Computational modeling and solution thermodynamics. *J. Therm. Anal. Calorim.* **2020**. [[CrossRef](#)]

42. Ruidiaz, M.A.; Delgado, D.R.; Martínez, F.; Marcus, Y. Solubility and preferential solvation of indomethacin in 1,4-dioxane + water solvent mixtures. *Fluid Phase Equilib.* **2010**, *299*, 259–265. [[CrossRef](#)]
43. Hildebrand, J.H.; Prausnitz, J.M.; Scott, R.L. *Regular and Related Solutions*; Van Nostrand Reinhold: New York, NY, USA, 1970.
44. Manrique, Y.J.; Pacheco, D.P.; Martínez, F. Thermodynamics of mixing and solvation of ibuprofen and naproxen in propylene glycol + water cosolvent mixtures. *J. Sol. Chem.* **2008**, *37*, 165–181. [[CrossRef](#)]
45. Holguín, A.R.; Rodríguez, G.A.; Cristancho, D.M.; Delgado, D.R.; Martínez, F. Solution thermodynamics of indomethacin in propylene glycol + water mixtures. *Fluid Phase Equilib.* **2012**, *314*, 134–139. [[CrossRef](#)]
46. Krug, R.R.; Hunter, W.G.; Grieger, R.A. Enthalpy-entropy compensation. 2. Separation of the chemical from the statistic effect. *J. Phys. Chem.* **1976**, *80*, 2341–2351. [[CrossRef](#)]
47. Apelblat, A.; Manzurola, E. Solubilities of o-acetylsalicylic, 4-aminosalicylic, 3,5-dinitrosalicylic and p-toluic acid and magnesium-DL-aspartate in water from T = (278–348) K. *J. Chem. Thermodyn.* **1999**, *31*, 85–91. [[CrossRef](#)]
48. Manzurola, E.; Apelblat, A. Solubilities of L-glutamic acid, 3-nitrobenzoic acid, acetylsalicylic, p-toluic acid, calcium-L-lactate, calcium gluconate, magnesium-DL-aspartate, and magnesium-L-lactate in water. *J. Chem. Thermodyn.* **2002**, *34*, 1127–1136. [[CrossRef](#)]
49. Yalkowsky, S.H.; Roseman, T.J. Solubilization of drugs by cosolvents. In *Techniques of Solubilization of Drugs*; Yalkowsky, S.H., Ed.; Marcel Dekker Inc.: New York, NY, USA, 1981; pp. 91–134.
50. Sotomayor, R.G.; Holguín, A.R.; Romdhani, A.; Martínez, F.; Jouyban, A. Solution thermodynamics of piroxicam in some ethanol + water mixtures and correlation with the Jouyban–Acree Model. *J. Sol. Chem.* **2013**, *42*, 358–371. [[CrossRef](#)]
51. Jouyban, A. Review of the cosolvency models for predicting solubility of drugs in water-cosolvent mixtures. *J. Pharm. Pharm. Sci.* **2008**, *11*, 32–58. [[CrossRef](#)]
52. Sardari, F.; Jouyban, A. Solubility of nifedipine in ethanol + water and propylene glycol + water mixtures at 293.2 to 313.2 K. *Ind. Eng. Chem. Res.* **2013**, *52*, 14353–14358. [[CrossRef](#)]
53. Khoubnasabjafari, M.; Shayanfar, A.; Martínez, F.; Acree, W.E., Jr.; Jouyban, A. Generally trained models to predict solubility of drugs in carbitol + water mixtures at various temperatures. *J. Mol. Liq.* **2016**, *219*, 435–438. [[CrossRef](#)]
54. Nozohouri, S.; Shayanfar, A.; Cardenas, Z.J.; Martinez, F.; Jouyban, A. Solubility of celecoxib in N-methyl-2-pyrrolidone + water mixtures at various temperatures: Experimental data and thermodynamic analysis. *Korean J. Chem. Eng.* **2017**, *34*, 1435–1443. [[CrossRef](#)]

Sample Availability: Samples of the compound ECT is available from the authors.



© 2020 by the authors. Licensee MDPI, Basel, Switzerland. This article is an open access article distributed under the terms and conditions of the Creative Commons Attribution (CC BY) license (<http://creativecommons.org/licenses/by/4.0/>).